Damping for the rotation of nonspherical DEM-solids

○ D. Krengel, The University of Electro-Communications, 182-8585 Chofu Chofugaoka 1-5-1 Tokyo, krengel@matuttis.mce.uec.ac.jp
H.-G. Matuttis, The University of Electro-Communications, 182-8585 Chofu Chofugaoka 1-5-1 Tokyo, hg@mce.uec.ac.jp

In discrete element (DEM) simulations of hard particles with soft contacts, for elongated particles the noise in the angular motion can introduce force changes which act on the rectilinear degrees of freedom for elastic interactions alone. At least for round particles with tangential forces (friction), this problem exists also. Independent damping forces at the particle contacts can neither damp away the motion due to these force fluctuations nor can they damp out the noise in the angular degrees of freedom. The resulting vibration leads to a slow creep downwards for the center of mass of granular aggregates. We discuss the similarities and differences for the damping of rectilinear and angular degrees of freedom and approaches for a rotational damping to decrease such creep.

1. Introduction

The common approach for discrete-element simulations (DEM) uses "hard-particles, soft-contacts". That means that the forces are computed from the geometrical overlap of the undeformed shapes, while the equations of motion are integrated out under the assumption of rigid particle shapes, see section A. However, as there are no point contacts, but extended overlap areas, a particles' rotation changes the magnitude and direction of the interparticle forces(1).

For a system where rectilinear motion alone is allowed, in mechanical equilibrium the residual noise can be compensated by a velocity dependent damping (Fig. 1, blue line). However, for a system with angular degrees of freedom and extended (instead of point-like) contacts, residual angular motion leads to inconsistencies in the force direction: Within a timestep τ, the orientation of the contacts can change by an angular increment $\Delta\varphi$ (Fig. 2) due to noise-like error in the orientation. Even if the overlap area may remain the same, the direction fluctuation leads to inconsistencies in the computation of the force equilibrium. As consequence, the velocity dependent damping for the rectilinear degrees of freedom can no longer compensate the residual motion and the noise in the angular degrees of freedom spreads towards the rectilinear degrees of freedom.

Simulations of particle configurations which should be static reveal persistent, small, noisy vibration amplitudes around the equilibrium positions(2). This vibration affects on the granular assembly like an external excitation, so for a granular heap or a granular assembly in a box, the height of the center of mass decays during the whole simulation time, instead of the expected decay of the kinetic (vibration) energy to zero. The imperfect force balance around the equilibrium of position and orientation induces a fluctuating numerical error on the scale of the timestep and the particle overlap. While it decays with the timestep (Fig. 3) nobody will be inclined to reduce the timestep and computational cost only to deal with that noise.

For elongated particles, the effect occurs already for elastic forces alone, for round particles only when tangential forces (friction) are present. Changing the friction laws does not remove the noise. "Numerically exact" friction,see (3) for a detailed description, based on the static friction constraints or even approaches like the Cundall-Strack friction model show noise induced by particle rotation. Figure 4 shows persistent oscillations in the kinetic energy of a granular heap also in simulations with the Cundall-Strack friction model, and irregular noise in the kinetic energy with a constraint-based friction model.

For configurations where the contacts should be static, it is therefore desirable to have an angular damping in addition to the damping in the rectilinear degrees of freedom.

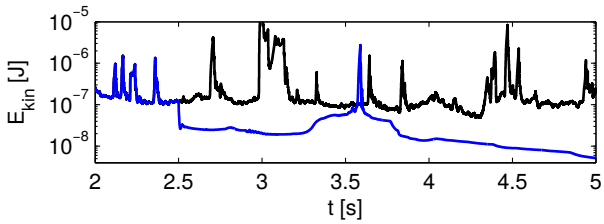

Fig. 1: Physically realistic decay of the average kinetic energy for a DEM-system with (unphysically) frozen out degree of freedom (blue line) and unphysical stagnation of the kinetic energy for the same system with (physical) intact rotation. Spikes indicate sudden reordering of the configuration under vibration. Computations with the numerically exact multibody friction from(3).

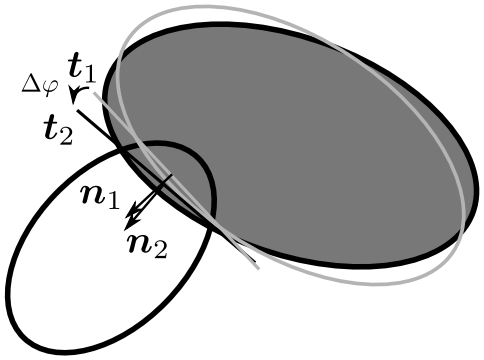

Fig. 2: In mechanical equilibrium, the forces and torques in a DEM-simulation should be balanced. Residual angular motion can induce small changes in the contact orientation $\Delta\varphi$. As consequence, the contact forces change, equilibrium is no longer maintained and the rectilinear degrees of motion experience noise.

2. Rotational damping

For the angular motion, there is no "actio = reactio" principle as there is for rectilinear motion. Introducing a damping torque where force components are microscopically not exactly balanced. Therefore, such a law will not violate any mechanical theorems.

For every contact j of a particle i we can compute an individual "damping torque", based on the relative tangential velocity at the point of contact $\mathbf{v}_{T,\mathrm{rel}}$ as

$$T_j^{\mathrm{damp}} = \mp\gamma_t\sqrt{I_i Y}|\mathbf{r}\times\mathbf{v}_{\mathbf{T},\mathrm{rel}}|, \qquad (1)$$

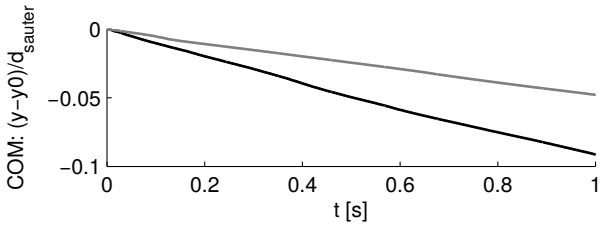

Fig. 3: Decay of the center of mass for the granular heap(3) in Fig. 8 in Sauter diameter with a timestep of $\tau = 10^{-5}$ (black). Using half the timestep (gray) decreases the creep.

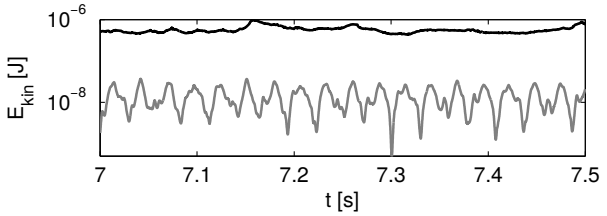

Fig. 4: Periodic oscillations in the kinetic energy for the simulation of the granular heap in Fig. 8 using the Cundall-Strack model (grey). Shown in black is the kinetic energy for the same heap using a non-stabilized constraint-based friction model(3).

with the sign depending on the direction of the contact vector $\mathbf{r}$ with respect to contact orientation. γ_t is a rotational damping coefficient, I_i the moment of inertia and Y the Youngs' modulus. For both contacting particles a, b we can then take the mean,

$$T_j^{\text{damp}} = \text{mean}(|T_{aj}^{\text{damp}}|, |T_{bj}^{\text{damp}}|), \tag{2}$$

oriented in the original direction

$$T_{aj}^{\text{damp}} = \text{sgn}(T_{aj}^{\text{damp}}) T_j^{\text{damp}}, \tag{3}$$

$$T_{bj}^{\text{damp}} = \text{sgn}(T_{bj}^{\text{damp}}) T_j^{\text{damp}}, \tag{4}$$

as the damping torque resulting from this contact. As the damping torques are reactive forces, it is not possible to simply sum up the contributions of every contact for each particle and hope that the resulting torques still compensate the noise in the angular motion. With multiple contacts, positive and negative damping torques are possible and the torques may compensate each other, i.e. the damping would be too small. Furthermore, it is not possible to decide the damping torque at each contact individually, as the rotation of the particle is influenced by the sum of all damping torques from all contacts.

For every single contact of a particle we can cumulate the individual damping torques, weighted by the elastic normal force $F_j^{n,\text{elast}}$ of the corresponding contact,

$$T_i^{\text{damp,sum}} = \sum_j T_j^{\text{damp}} |F_{N,j}^{\text{elast}}|, \tag{5}$$

With this value we can obtain the total damping torque per particle as

$$T_i^{\text{damp,tot}} = \frac{n_i T_i^{\text{damp,sum}}}{\sum_j |F_{N,j}^{\text{elast}}|}, \tag{6}$$

where n_i is the number of contacts the particle has. This damping torque has to compensate the elastic torque T^{elast} and the particles own rotation ω_i, while the rotation of a surrounding particle matrix $\overline{\omega}^0$ (Fig. 5) imposes an upper limit on the damping torque, i.e. it has to compensate the term

$$\widetilde{T}_i = T_i^{\text{elast}} + I_i \frac{\omega_i - \omega_i^0}{\tau}. \tag{7}$$

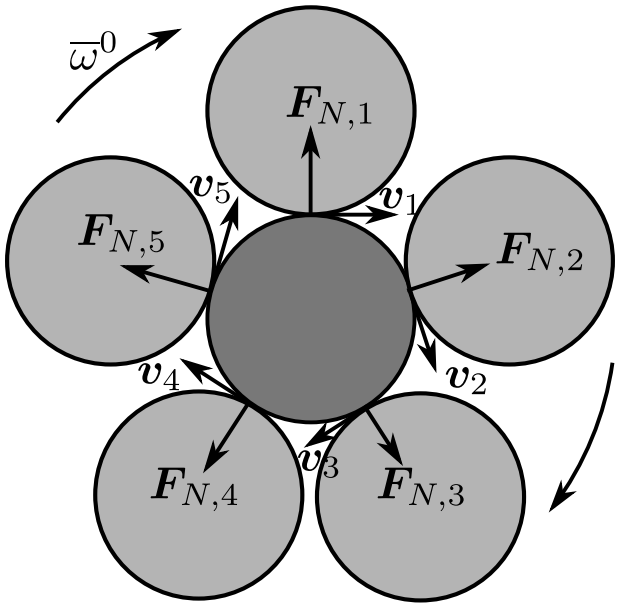

Fig. 5: The rotation of a surrounding granular matrix imposes an upper limit $\overline{\omega}^0$ on the damping torque of each individual particle. In mechanical equilibrium, the particle itself follows the rotation of the surrounding matrix and $\omega = \overline{\omega}^0$.

In mechanical equilibrium, the rotation of a particle will be so that the tangential velocities at all contacts average to zero. We obtain the elastic torque from the elastic forces at each individual contact,

$$T^{\text{elast}} = r_x F_y^{\text{elast}} - r_y F_x^{\text{elast}}, \tag{8}$$

with an elastic force

$$\mathbf{F}^{\text{elast}} = F_N^{\text{elast}} \cdot \mathbf{n} + F_T^{\text{fric}} \cdot \mathbf{t}. \tag{9}$$

The total elastic torque can then be obtained by simple summation of the individual damping torques from all contacts.

Determination of the rotation from the surrounding particle matrix, i.e. $\overline{\omega}^0$ works analogous to the damping torque, as the sum of weighted partner angular velocities,

$$\overline{\omega}_i^0 = \frac{\sum_j \omega_j |F_{N,j}^{\text{elast}}|}{\sum_j |F_{N,j}^{\text{elast}}|}, \tag{10}$$

where

$$\omega_j = \frac{\mathbf{r}_j \times \mathbf{v}_{T,\text{rel},j}}{|\mathbf{r}_j|^2} \tag{11}$$

is the relative rotation of the contact.

As the magnitude of the damping torque can not be greater than the magnitude of the elastic torque, we introduce a cutoff

$$(\widetilde{T}_i + T_i^{\text{damp,tot}}) \cdot \widetilde{T}_i < 0 : T_i^{\text{damp,tot}} = -\widetilde{T}_i. \tag{12}$$

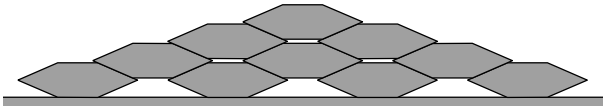

Fig. 6: Ten hexagonal particles with radius 5cm stacked with upper particles in the gaps between lower particles.

The final torque acting upon the particle is then given by

$$T = T_i^{\text{phys}} + T_i^{\text{damp,tot}}, \tag{13}$$

where T^{phys} is the torque resulting from the full interaction forces.

3. Numerical applications

In the following we apply our algorithm to some sample problems and compare the results with the undamped versions. Through all simulations we use the parameters in table 1 with a timestep of $\tau = 10^{-5}$, except when explicitly stated otherwise.

Young's modulus	10^7[N/m]
Normal damping coefficient γ	0.5
Rotation damping coefficient γ_T	0.1
Coefficient of friction μ	0.6
(particle-particle, particle-wall)	
Density of particles σ	5000[kg/m^2]

Tab. 1: Parameters for the interaction computation of two-dimensional polygonal particles.

3.1 Cannonball-stacking

For a wedged stack of 10 identical hexagonal particles, as shown in Fig. 6, the situation is rather simple: While the friction between the particles is keeping the stack stable, residual energy stored in the rotational degrees of freedom in form of long-wave oscillations, is continuously transferred into the rectilinear degrees of freedom and only slowly dissipated by the linear damping mechanisms. If we include our rotational damping, we find an offset in the creep to higher values (Fig. 7), i.e. the onset of creep is delayed compared with the undamped version. As the configuration is fairly stable, most of the remaining energy had already been dissipated before, and the net benefit is small.

3.2 Granular heaps

For a granular heap of polygonal particles with shape and size dispersion, like in Fig. 8, the situation is more complicated. The variation in size and shape means, that more energy modes remain in the rotational degrees of freedom that need to be accounted for.

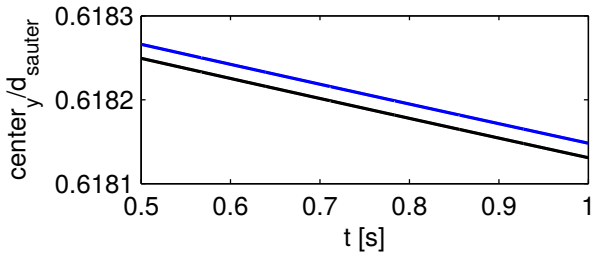

Fig. 7: Center of mass height of the stack in Fig. 6 in its static phase. The case without rotational damping is shown in black, with additional rotational damping in blue.

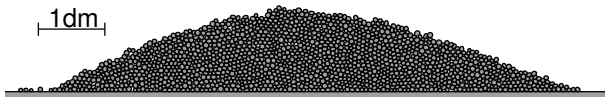

Fig. 8: Granular heap of 1622 particles in a static configuration.

If we compare the relative drift of the centre of mass (Fig. 9), scaled in Sauter mean diameter,

$$d_{\text{Sauter}} = 2\sqrt{A}/\pi, \tag{14}$$

we find, that the drift starts to decrease slightly after some time for the version with additional rotation damping. If we vary the damping parameter γ_T from equation (5), we find an optimum between $\gamma_T = 0.05$ and $\gamma_T = 0.5$, see Fig. 10. Too large values for γ_T lead to overcompensation of the damping torque and subsequent increase of the residual angular velocity, while for too small values, the effect of the damping torque becomes simply too small to make a difference. If the timestep is reduced, then the numerical noise and error in $\Delta\varphi$ decrease as well, and the position drift becomes smaller (Fig. 11).

4. Conclusion

In section 1., we have shown how residual angular motion can lead to errors in the contact orientation and induce persistent noise in the rectilinear degrees of freedom that velocity dependent linear damping forces cannot compensate. To reduce this noise we have presented a novel damping formalism for the angular degrees of freedom in section 2.. While it follows the general structure of damping in the normal contact forces(1), unlike normal damping, angular damping can not be treated independently for each contact of a particle, but has to consider cumulative values instead. Finally, in section 3. we have applied the damping formalism to two sample cases and discussed its difference with the undamped case.

A The Discrete Element Method

The dynamics of rigid particles largely depend on their shape: For round particles friction is subdued, they can "escape" via rolling. On the other hand, angular particles are more likely to slide, making static friction effective. For the DEM in general, relative velocities and accelerations are required instead of absolute values. For elongated particles, forces are no longer central, the contacts can be arbitrarily oriented and the resulting torques must be included in the calculations.

We choose the overlap polygon, as shown in Fig. 12, as a measure of physical deformation of actual particles. We can find the overlap area A from the intersection points S_1 and S_2, and as a force point P the centroid of the overlap area. The connecting line between S_1 and

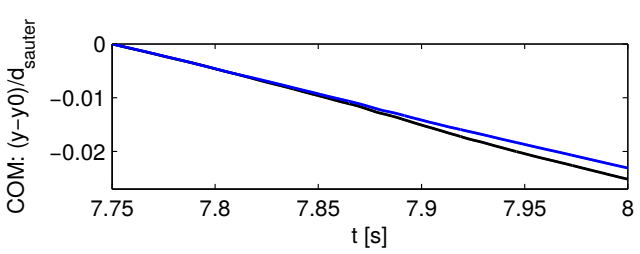

Fig. 9: Drift in the centre of mass for the heap in Fig. 8 in Sauter diameter. Shown in black is the version without rotation damping, shown in blue the version with our rotation damping.

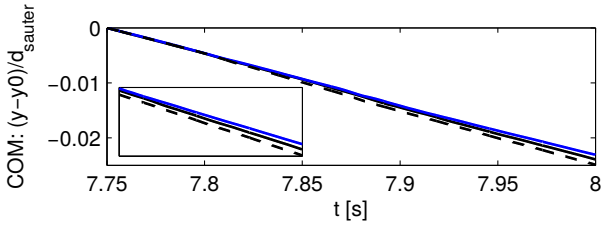

Fig. 10: Change of the vertical center of mass drift for the heap in Fig. 8 with rotational damping in dependence of the damping parameter γ_T. Shown in a solid black line is $\gamma_T = 0.05$, in a solid blue line is $\gamma_T = 0.1$, and in a dashed black line is $\gamma_T = 0.5$.

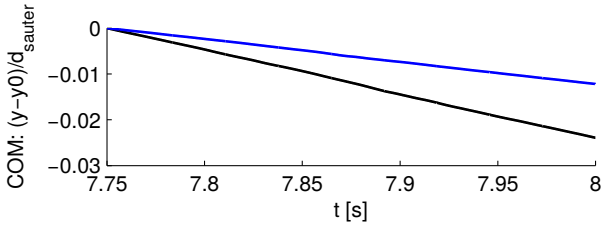

Fig. 11: Change of the vertical center of mass drift for the heap in Fig. 8 in dependence of the timestep τ. Shown in a solid black line is $\tau = 10^{-5}$, and in a solid blue line is half the timestep, $\tau = 5 \cdot 10^{-6}$.

S_2 defines the tangential direction $\mathbf{t}$, which also fixes the normal direction $\mathbf{n}$. The reduced mass m is given by the masses m_a,m_b via

$$\frac{1}{m} = \frac{1}{m_a} + \frac{1}{m_b}. \tag{15}$$

The elastic force

$$F^{\mathrm{el}} = \frac{YA}{l} \tag{16}$$

(with the Youngs modulus Y in units of [N/m]) acts in normal direction, proportional to the overlap area. The characteristic length

$$l = \frac{4|\mathbf{r}_a||\mathbf{r}_b|}{|\mathbf{r}_a| + |\mathbf{r}_b|} \tag{17}$$

allows to define the elastic force in units of [N]. The normal dissipative force is chosen proportional to the

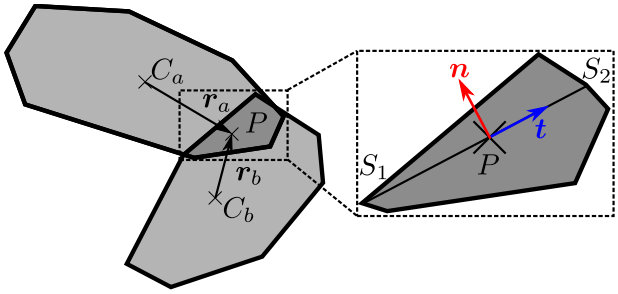

Fig. 12: Contact geometry for two polygons (light grey) and their overlap polygon (dark grey), showing the centers of mass C_a, C_b, the center of mass for the overlap polygon P, and the contact vectors r_a, r_b from the centers of mass to the center of the overlap (left). The inset (right) shows (exaggerated) the normal ($\mathbf{n}$) and the tangential ($\mathbf{t}$) direction.

change of A/l as

$$F^{\mathrm{diss}} = \gamma\sqrt{mY}\frac{\dot{A}}{l}, \tag{18}$$

with a damping constant γ. Solid friction is implemented in tangential direction. Lastly, the torques are computed as

$$\mathbf{T} = \mathbf{r} \times \mathbf{F}, \tag{19}$$

with the sum of all normal and tangential forces $\mathbf{F}$.

References

(1) Matuttis, H.G. and Chen, J., "Understanding the discrete element method", Wiley (2014)

(2) Chen, J., "Discrete element method for 3D simulations of mechanical systems of non-spherical granular materials", PhD-Thesis, The University of Electro-Communications (2012)

(3) Krengel, D. and Matuttis, H.-G., "Implementation of static friction for many-body problems in two-dimensions", to appear in Journal of the Physical Society of Japan